

A climatological perspective of water vapor at the UTLS region over different global monsoon regions: observations inferred from the Aura-MLS and reanalysis data

K. N. Uma · Subrata Kumar Das · Siddarth Shankar Das

Received: 12 March 2013 / Accepted: 10 February 2014 / Published online: 19 February 2014
© Springer-Verlag Berlin Heidelberg 2014

Abstract The Aura-MLS observations of eight years from 2004 to 2011 have been utilized to understand the hydration and the dehydration mechanism over the northern and the southern hemispheric monsoon (NH and SH) regions. The monsoon regions considered are the Asian Summer Monsoon, East Asian Summer Monsoon, Arizona Monsoon (AM), North African Monsoon, South American Monsoon and the Australian Monsoon. The annual cycle of water vapor as expected shows maxima over the NH during June–August and during December–February over the SH. The time taken by the air parcels over the NH monsoon regions is found to be different compared to that over the SH monsoon regions. The analysis shows the concentration of water vapor in the upper troposphere and the lower stratosphere (UTLS) has not changed over these eight years in both the hemispheres during their respective monsoon seasons. The present analysis show different processes viz., direct overshooting convection, horizontal advection, temperature and cirrus clouds in influencing the distribution of water vapor to the UTLS over these different monsoon regions. Analysis of the UTLS water vapor with temperature and ice water content shows that the AM is hydrating the stratosphere compared to all the other monsoon regions where the water vapor is getting dehydrated. Thus it is envisaged that the present results will have important implications in understanding the exchange

processes across the tropopause over the different monsoon regions and its role in stratosphere chemistry.

Keywords Stratospheric water vapor · UTLS · Monsoon · Aura-MLS

1 Introduction

Water vapor plays a key role in controlling the chemical, radiative and dynamic processes in the atmosphere. Its main role lies in the formation of clouds and precipitation, which in turn govern the Earth's weather and climate system. It has important impacts on atmospheric circulations through latent heat exchanges and redistribution of energy (Schneider et al. 2010). The distribution of water vapor is strongly influenced by both the large-scale circulation and localized convection. There has been a renewing scientific attention towards the transport of water vapor and the factors that control its transport from the troposphere to the stratosphere and vice versa. An increase in stratospheric water vapor tends to cool the stratosphere and warm the troposphere and also enhance the rate of ozone destruction (Dvortsov and Solomon 2001; Shindell 2001; Rosenlof et al. 2001; Solomon et al. 2010; Wright et al. 2011; Das 2009; Randel et al. 2012).

The entry pathways that govern the transport of water vapor into the stratosphere have to be understood in detail. Brewer (1949) postulated the first hypothesis for dryness of tropical stratosphere, which is limited to tropics where the tropopause is cold enough to freeze dry the air. The tropical tape-recorder effect has been explained by Mote et al. 1996, where the stratospheric water vapor exhibits a strong seasonal cycle. However, (Newell and Gould Stewart 1981, hereafter NG81) pointed out that to be occurring in

K. N. Uma (✉) · S. S. Das
Space Physics Laboratory, Vikram Sarabhai Space Centre,
ISRO-Department of Space, Government of India,
Trivandrum 695022, India
e-mail: urmi_nmrf@yahoo.co.in; uma_kn@vssc.gov.in

S. K. Das
PM & A Division, Indian Institute of Tropical Meteorology,
Pune 411008, India

preferential seasons and regions, over the Bay of Bengal (BoB) during boreal-summer, and western Pacific during boreal-winter. The two different processes that govern the entry of water vapor into the stratosphere is (1) the direct convective injection and (2) slow diabatic ascent, a way by freeze-drying (Holton et al. 1995; Holton and Gettelman 2001; Gettelman et al. 2002; Fueglistaler et al. 2005; Rao et al. 2008; Uma et al. 2013 and references therein).

In this context, the South Asian summer monsoon is considered to be a region of interest, as it is characterized by persistent water vapor maximum extending from 150 to 68 hPa (Park et al. 2007). Global model analysis results show that convection in the southeast monsoon region is primary contributor to the moist phase of the tropical Tape-Recorder (Bannister et al. 2004; Lelieveld et al. 2007). Extended studies have been made to understand the monsoon convection over the South Asian region and the Bay of Bengal (Petersen and Rutledge 2001; James et al. 2008; Devasthale and Fueglistaler 2010). Studies have even been carried out over the coastal and maritime convection in the vicinity of south China and Philippine seas (Petersen and Rutledge 2001; Hirose and Nakamura 2005; James et al. 2008). Many studies have also focused on the continental convection over the Tibetan plateau and its role in the stratospheric water vapor (Uyeda et al. 2001; Fujinami et al. 2005; Fu et al. 2006, Yasunari and Miwa 2006). Uma et al. (2013) have studied the climatological characteristics of water vapor intrusion into the stratosphere over the North Bay of Bengal and East Equatorial Indian Ocean. The authors have shown that the North Bay of Bengal region play an active role in hydrating rather than dehydrating the lower stratosphere. Hence considerable debate is still on in understanding the relative contributions of the convection over these regions into the transport of water vapor into the stratosphere.

It is well understood that the above studies have concentrated in and around the South East Asian summer monsoon. It is equally important to understand the transport of water vapor in different monsoon regions like Australian monsoon (Davidson et al. 1983), North African monsoon (Hastenrath 2000), Arizona monsoon (Adams and Comrie 1997) and South American monsoon (Zhou and Lau 1999). The main reason for this understanding is that the monsoons are one of the key elements that define the features of Earth's climate. They strongly affect the agriculture and hence in turn the global economy. The water vapor is the main component of all the monsoon systems which controls the formation of deep convection and hence transport. The main intent of this communication is to understand the transport of water vapor in different monsoon regions, which is very crucial to understand the role of each monsoon region in transport processes in the upper tropospheric and lower stratospheric (UTLS) region. It is

envisaged that the present analysis will shed some light in understanding the exchange processes in context with different monsoon regions.

To address the above scientific issues, the information of the UTLS water vapor is required. The water vapor in the UTLS region is difficult to detect due to its large variability and smaller magnitudes and also difficult to accurately determine its concentration at that height region. The global coverage of water vapor is possible only through spaceborne measurements [e.g. Aura-Microwave Limb Sounder (MLS)], though the temporal resolution is poor but provides a better opportunity for simultaneous global measurements of water vapor in the UTLS region. At this juncture, these observations can be much useful to explore the stratosphere-troposphere exchange (STE) processes.

2 Data analysis

The MLS on-board the Aura satellite provides simultaneous global measurements of various chemical species including water vapor in the lower and middle atmosphere. The Aura-MLS observes thermal microwave–far infrared emission from the Earth's atmosphere in 5-spectral regions. The water vapor measurement described in this study is from Version 3.3-Level 2 retrieved from measurements of the 183 GHz H₂O rotational line spectrum (Livesey et al. 2011). The Aura-MLS observations are available at different pressure levels and the data are useful from 316 to 0.002 hPa. The vertical resolution for water vapor measurements is in the range 2.0–3.7 km from 316 to 0.22 hPa and degrades to 6–11 km for pressures lower than 0.22 hPa. The along track horizontal resolution is ~210–360 km for pressures greater than 4.6 hPa, and degrades to 400–740 km at lower pressures. The horizontal cross-track resolution is the 7 km full width half maximum of the MLS 190-GHz field-of-view for all pressures and ~200–300 km along track (Read et al. 2007; Lambert, et al. 2007). The data span of the present study is from August 2004 to December 2011. In our analysis we filtered the data based on the criteria of precision values, quality and convergence field and profile status. More details about the instrument, algorithms and science products can be found in Waters et al. (2006) and also in the website <http://mls.jpl.nasa.gov>. For water vapor, typical single profile precisions are 0.9, 0.7, 0.5, and 0.3 ppmv at 215, 147, 100 hPa, lower stratosphere, respectively (Livesey et al. 2011). For water vapor, typical single profile precisions are 0.9, 0.7, 0.5, and 0.3 ppmv at 215, 147, 100 hPa, lower stratosphere, respectively (Livesey et al. 2011). The typical estimated precision of the temperature measurement is ~1 K at 100 hPa (Froidevaux et al. 2006). The water vapour mixing ratio and temperature retrieved from the

MLS are validated and can be found in Lambert et al. (2007) and Schwartz et al. (2008), respectively.

We used the NOAA interpolated Outgoing Long wave Radiation (OLR) to quantify the convection and this data are real-time satellite observations and downloaded from website http://www.esrl.noaa.gov/psd/data/gridded/data.interp_OLR.html. The daily mean OLR data are gridded for $2.5^\circ \times 2.5^\circ$ spatial resolution. Detail description of the NOAA interpolated OLR data set is described in Liebmann and Smith (1996). Less than 220 W m^{-2} is used to indicate the presence of deep convection (Das et al. 2011 and references therein). For vertical velocity ERA-Interim reanalysis data are used. The ERA-Interim (Dee et al. 2011) is the latest global atmospheric reanalysis produced by the European Centre for Medium-Range Weather Forecasts (ECMWF). The spatial and temporal resolutions of the ERA-Interim reanalysis data are $1.5^\circ \times 1.5^\circ$ and every 6 h, respectively and the data is downloaded from the website http://data-portal.ecmwf.int/data/d/interim_daily/levtype=pl/. Data are available at the different pressure and isentropic levels. Detail bias correction, accuracy and limitation of the ERA-Interim reanalysis data can be found in Dee et al. (2011) and comprehensive documentation is available in the website <http://www.ecmwf.int/publications/newsletters>.

3 Results

Figure 1 shows the location of the monsoon regions considered for the present study. The regions have been divided based on the study reported by Zeng and Lu (2004). They have used an objective criterion to define globally unified monsoon onset and retreat for the first time using precipitable water vapor. Six monsoon regions have been classified (1) Asian summer monsoon (10°N – 26°N ; 70°E – 105°E) (hereafter ASM) (2) East Asian summer monsoon (10°N – 30°N ; 105°E – 150°E) (hereafter EASM) (3) North American or the Arizona monsoon (10°N – 30°N ; 90°W – 110°W) (hereafter AM) (4) North African monsoon (10°N – 20°N ; 30°W – 25°E) (hereafter NAM) (5) South American monsoon (15°S – 25°S ; 40°W – 65°W) (hereafter SAM), and (6) Australian monsoon (10°S – 20°S ; 120°E – 150°E) (hereafter AUM). Details are listed in Table 1. Figure 2 shows the seasonal mean, i.e., December–January–February (DJF), March–April–May (MAM), June–July–August (JJA), and September–October–November (SON) of interpolated NOAA outgoing long wave radiation (OLR) averaged from 2004 to 2011. During JJA, OLR less than 200 W m^{-2} is observed over the ASM, EASM, NAM and AM and during DJF it is observed over SAM and AUM and it is well expected and well reported. This shows that deep convective clouds are situated over these regions and

it is envisaged that the enormous amount of water vapor must be pumped up to and above the tropopause, which is reported earlier (Gettelman et al. 2002; Wang and Dessler 2012; Randel et al. 2012 and references therein).

Figure 3 shows the global distribution of seasonal mean (DJF, MAM, JJA, and SON) water vapor mixing ratio averaged from 2004 to 2011 obtained from the Aura-MLS satellite observations at 261 hPa. The closed contours in Fig. 3 shows the $\text{OLR} < 220 \text{ W m}^{-2}$. It shows that during DJF the concentration of water vapor is found to be between 400 and 500 ppmv over the Northern parts of Australia and western Pacific, South Africa and South America. However the concentration over the Australia is found to be greater than 500 ppmv, which is higher compared to other regions. During this period (DJF) the above regions experience their respective monsoon seasons, due to which the concentration of water vapor is found to be high. During MAM, the core of water vapor is located in the same regions (except Australia), with less concentration of about 300–350 ppmv. The concentration further decreased over the AUM region and found to be less than 200 ppmv. Water vapor is found to increase over the south and central Bay of Bengal during the above period. This is mainly due to the fact that pre-monsoon depressions occur during this period which considerably increases the concentration of water vapor. Low concentration of about 150–200 ppmv is observed over the adjoining oceans surrounding these continents. During JJA, the summer monsoon sets over the Indian and the East Asian continent, and the concentration is observed to be higher compared to other monsoon regions as clearly revealed from Fig. 3. The concentration is more than 500 ppmv and it is found to cover almost the South and East Asian region. The water vapor is found to be high over the North American region, where the Arizona monsoon sets during this period, however the concentration of water vapor is very less comparably to the East Asian continent. The North African monsoon constitutes low water vapor compared to the other northern hemispheric monsoon regions. During SON period, the concentration of water vapor almost resembles the MAM period, except for the high concentration over the Indian region. This is due to the retreating phase of monsoon otherwise called the north-east monsoon, occurs during the October–November period, which is also a source of water vapor. Over all the regions it is found to vary between 300 and 400 ppmv. Also, over the western and central pacific, the concentration is always high and due to the fact that the ascending branch of the Hadley cell is situated over these locations (NG, 81; Gettelman et al. 2002). The above discussion supports the existing evidences on the monsoon convection being the source of water vapor and the forthcoming section will discuss on the differences in the water vapor observed from 316 to 82 hPa

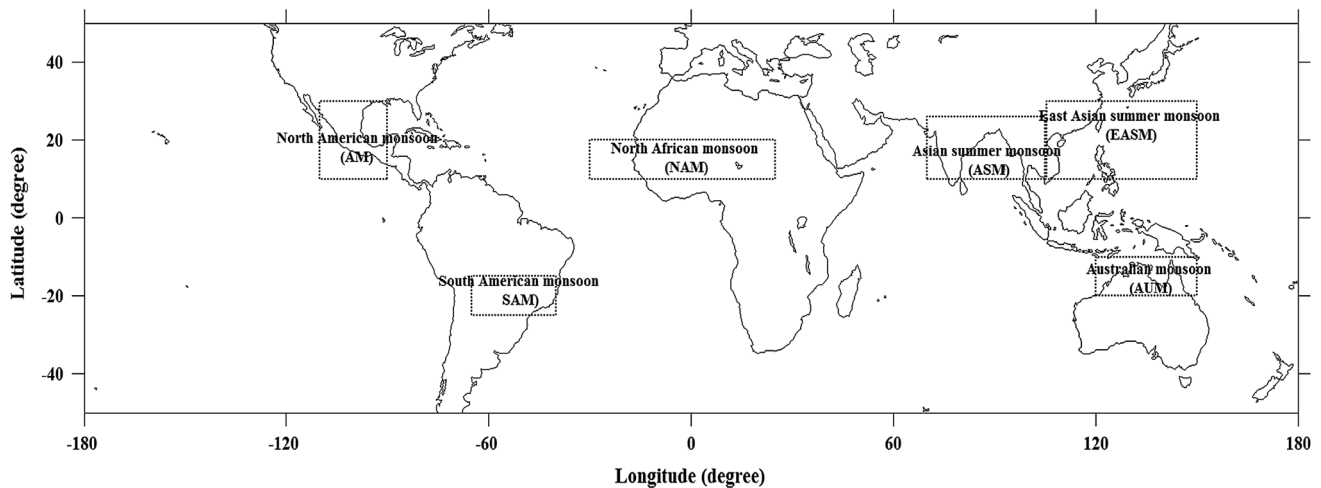


Fig. 1 Location of the monsoon regions considered for the present study. See text and Table 1 for details

Table 1 Detail list of monsoon region considered for the present study

Monsoon region	Abbreviation	Latitude	Longitude	Period
Asian summer monsoon	ASM	10°N–26°N	70°E–105°E	June–August
East Asian summer monsoon	EASM	10°N–30°N	105°E–150°E	June–August
North American monsoon (Arizona monsoon)	AM	10°N–30°N	90°W–110°W	June–August
North African monsoon	NAM	10°N–20°N	30°W–25°E	June–August
Australian monsoon	AUM	10°S–20°S	120°E–150°E	December–February
South American monsoon	SAM	15°S–25°S	40°W–65°W	December–February

over these monsoon regions in light of present understanding.

4 Discussion

Figure 4 shows the monthly variability of water vapor over different monsoon regions i.e., ASM, EASM, AM, NAM, AUM and SAM at 316, 147, 100 and 82 hPa. The water vapor exhibits strong annual cycle at all the pressure levels as explained by Mote et al. (1996), except at 316 hPa over the NAM and AM regions. Maximum water vapor is observed during JJA over the ASM, EASM and during DJF over SAM, AUM. The water vapor is almost constant and

found to be ~ 900 and ~ 750 ppmv at 316 hPa over AM and NAM, respectively. On the other hand at 316 hPa, the maximum water vapor is observed to be about 2,250, 1,100, 1,750 and 900 ppmv over ASM, EASM, AUM and SAM, respectively and follows a strong monthly variability. This clearly explains that the water vapor concentration is maximum over the ASM region during JJA compared to the other monsoon regions. It is interesting to note that even though in presence of convection ($OLR < 220 \text{ W m}^{-2}$) over other locations, the ASM region only have higher concentration of water vapor during JJA as clearly seen from Fig. 3. The temperature during JJA and DJF obtained from the ERA-Interim reanalysis data at 250 and 100 hPa is analysed in order to understand the water vapor distribution and it is shown in Fig. 5. Higher temperature ($>10\text{--}15 \text{ K}$) is observed over the ASM region during JJA at 250 hPa. This indicates that at this high temperature over the ASM, the holding capacity of water vapor is enhanced compared to other monsoon locations and seasons. This might be one of the probable reason for the ASM to have maximum water vapor in the upper troposphere during JJA. The temperature at 100 hPa over the ASM during JJA is very cool ($\sim 190 \text{ K}$) compared to other monsoon regions, which will be discussed in the forthcoming section. Hence the ASM is an area of scientific interest and there have been several studies, in particular on the transport of water vapor into the stratosphere over this region (Park et al. 2007; Randel et al. 2012; James et al. 2008; Uma et al. 2013). Thus, one expects that the ASM will transport more water vapor into the stratosphere compared to the other monsoon regions. To look into that aspect, let us consider the water vapor concentration at the other levels as shown in Fig. 4.

At 147 hPa, the concentration of water vapor as expected, is observed to be one order less than that

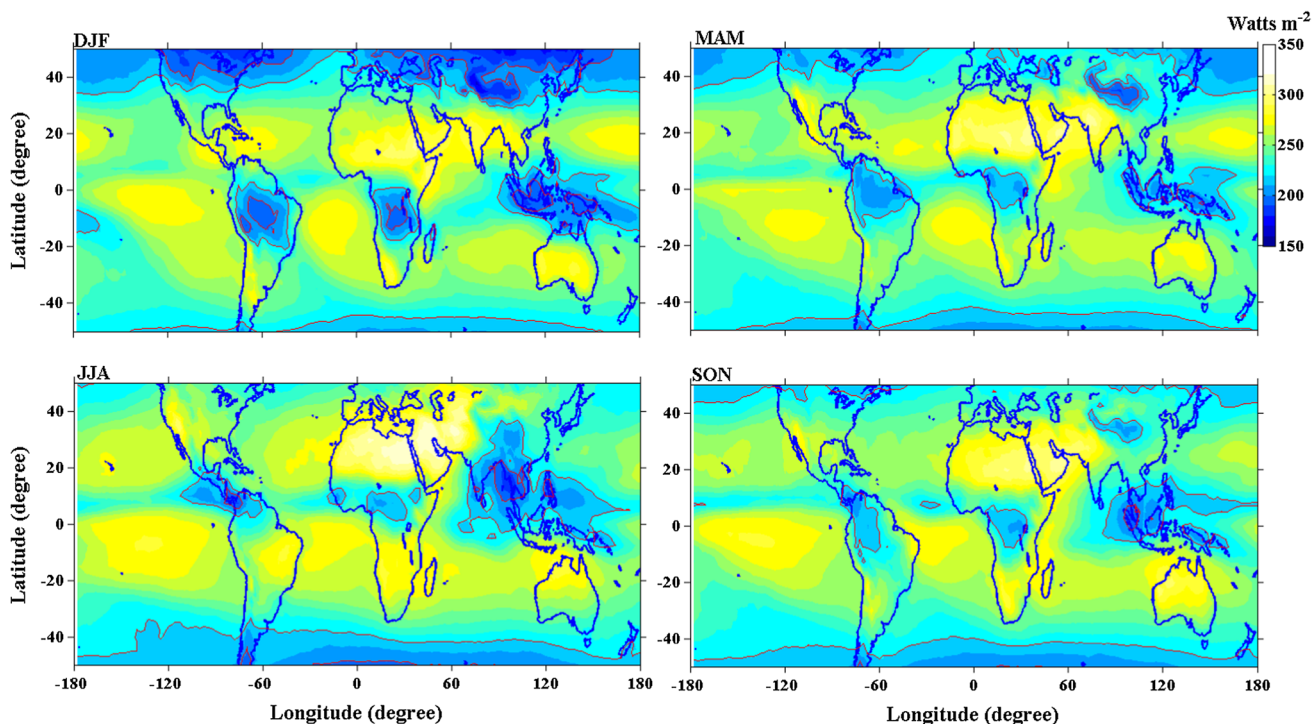


Fig. 2 Seasonal mean of outgoing long-wave radiation (OLR) averaged from 2004 to 2011 obtained from NOAA. *Closed red contours* indicate the OLR < 220 W m⁻²

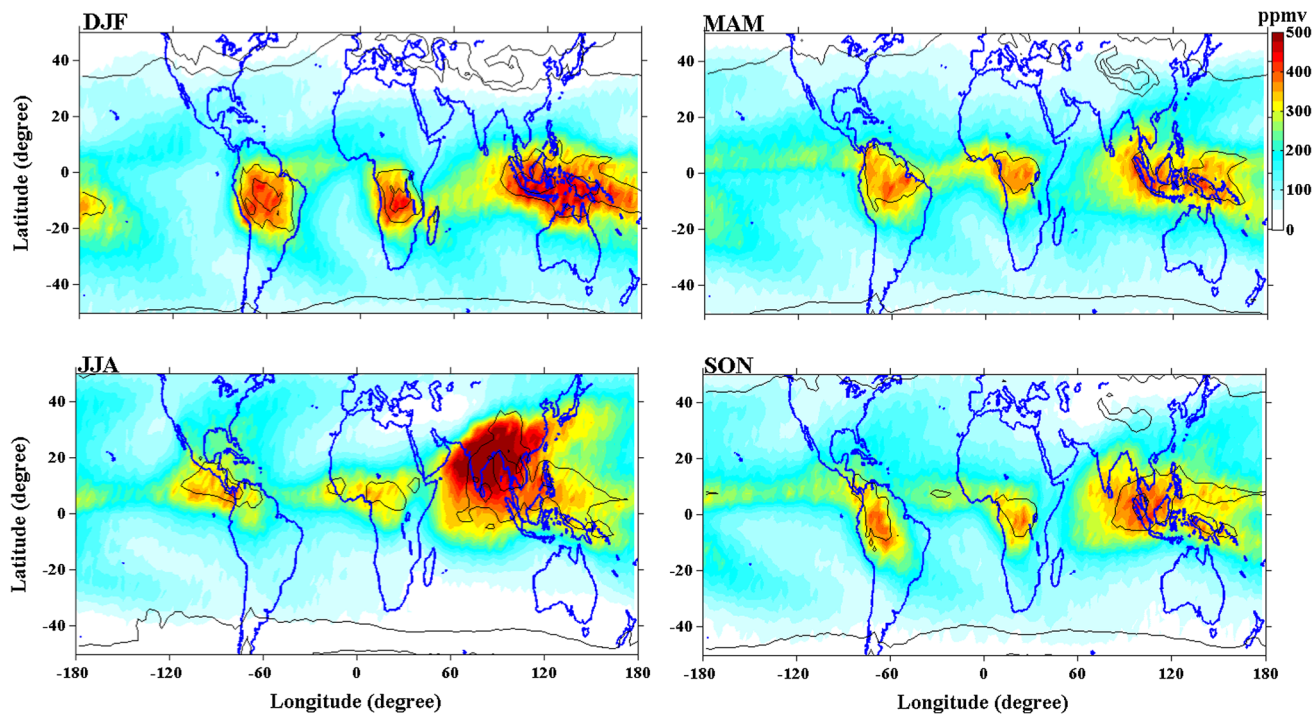


Fig. 3 Seasonal mean of water vapour mixing ratio averaged from 2004 to 2011 obtained from Aura-MLS at 261 hPa. *Closed black contours* indicate the OLR < 220 W m⁻²

observed at lower levels. It exhibits annual cycle and AUM and SAM does not show much variability in contrast to its lower level. The maximum water vapor is about 18, 15, 12,

12 ppmv, respectively over the ASM, EASM, AM and NAM. Over the SAM and AUM, it is found to vary between 10 and 15 ppmv at 147 hPa. This level is

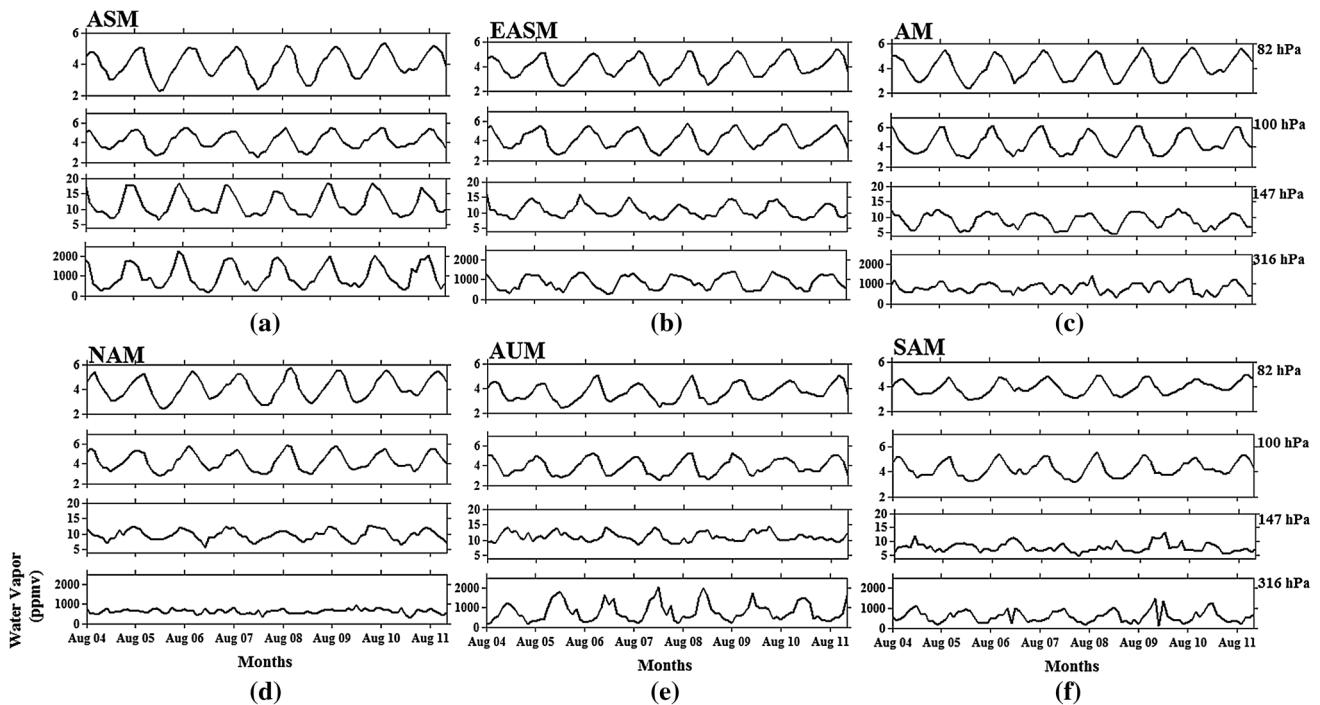


Fig. 4 Monthly variability of water vapour mixing ratio over **a** Asian summer monsoon (ASM), **b** East Asian summer monsoon (EASM), **c** North American or Arizona monsoon (AM), **d** North African

monsoon (NAM), **e** Australian monsoon (AUM), and **f** South American monsoon (SAM), respectively at 316, 147, 100 and 82 hPa

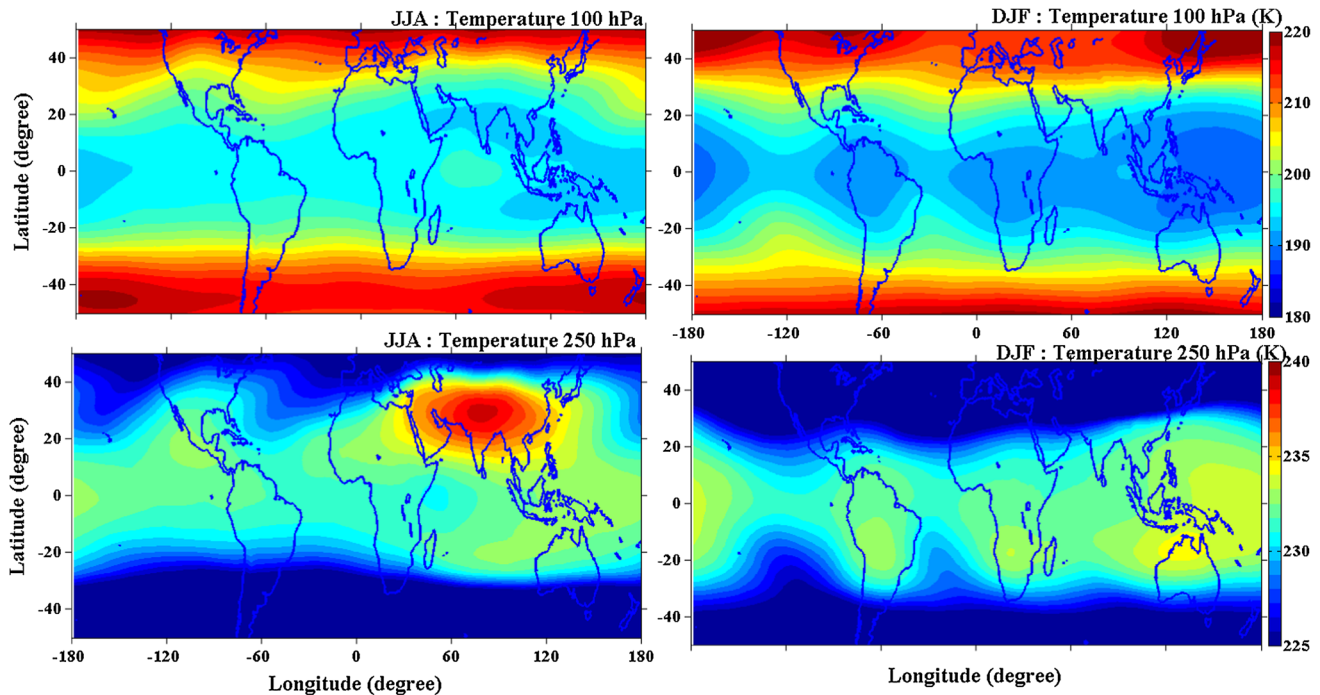


Fig. 5 Seasonal mean for JJA (*left panels*) and DJF (*right panels*) (2004–2011) of temperature at 250 and 100 hPa

considered to be the maximum level of neutral buoyancy in the tropics which is about 14 km. Rapid ascending air masses generated by deep convection can overshoot this

level and can reach up to the tropopause. The region between this two is called as the Tropical Tropopause Layer (TTL) (Fueglistaler et al. 2009). The processes that

govern the observed low concentrations of water vapor in the stratosphere cannot be explained unless the dehydration mechanism in the TTL is addressed (Brewer 1949; Dessler and Kim 1999; Holton and Gettelman 2001).

The water vapor at the top of the TTL exhibits annual cycle over all the monsoon regions, unlike at the other lower height levels. The concentration of water vapor is found to vary between 5 and 6 ppmv over all the 6-monsoon regions, irrespective to the difference in the availability of water vapor at the lower levels. Over the AM region, the water vapor is found to be 6 ppmv throughout all the years. It is also interesting to note that the maxima occur during the month of August over all the monsoon regions. This shows that the time taken for the parcels to reach the stratosphere is different for different hemispheric monsoon regions. Two different rates of air parcel were observed, i.e. one from 100 to 57 hPa and other from 57 to 31 hPa. In the NH monsoon regions, the air parcel take ~3.5 months to reach from 100 to 57 hPa and ~8.5 months to reach from 57 to 31 hPa. Whereas, over the SH monsoon region, the air parcel takes ~5 months to reach from 100 to 57 hPa and ~7.5 months from 57 to 31 hPa. This indicates that the rate of air parcel travelling from the tropopause to the lower stratosphere is faster than the middle stratosphere. It also appears that air parcel moves faster in the NH as that of SH in the lower stratosphere and vice versa in the middle stratosphere. With the available dataset, it is observed reveals that the concentration of water vapor in the UTLS region has not changed over these 8 years (2004–2009) and found to be almost constant during their respective monsoon seasons.

At 82 hPa, the concentration of water vapor is decreased by 0.5–1 ppmv compared to that it had at 100 hPa, over all the monsoon regions. This shows that only a little amount of water vapor gets dehydrated at the tropopause level and most of the times after dehydration at the bottom of TTL, the water vapor enters the stratosphere, with the same concentration that it had at the tropical tropopause. This aspect is discussed in terms of the water vapor, the tropopause temperature and saturation mixing ratio in the upcoming section. Within the TTL the amount of water vapor has been reduced from 12–18 to 4–6 ppmv. Also, the vertical transport of water vapor into the stratosphere over all the monsoon regions is the same irrespective of the availability of water vapor at the bottom of TTL. For example, the ASM where the availability of water vapour concentration is almost double compared to that of other monsoon regions, however, in the lower stratosphere the concentration remains same as that of other monsoon region where the concentration of water vapor at lower troposphere is very less. It also shows that the dehydration mechanism must be more over the ASM compared to other regions. The above aspects would be dealt by considering the role of tropopause temperature, vertical convection, and

horizontal advection in redistribution of lower stratospheric water vapor and role of ice formation at the UTLS region.

4.1 Role of tropopause temperature

Brewer (1949) postulated that air masses entering the stratosphere must pass through the low temperatures at the tropopause with substantial dehydration. As of now there are ample of observational and simulation studies relating the tropopause temperature and the dehydration of water vapor in the stratosphere (Mote et al. 1996; Gettelman et al. 2002; Liu et al. 2007; Flury et al. 2012; Uma et al. 2013). Thus, further analysis is carried out in this aspect by correlating the monthly variability of temperature at 100 hPa (T_{100}) with water vapor at 100 and 82 hPa. In addition, the saturation mixing ratio (γ_{satt}) is estimated from (Bolton 1980; Tetens 1930)

$$\gamma_{satt} = 0.623 \left(\frac{e_s}{p - e_s} \right) \tag{1}$$

where, the vapor pressure (e_s) is given by

$$e_s = 6.11 \times 10^{7.5 \left(\frac{T}{T+237.3} \right)} \tag{2}$$

and T is the absolute temperature, p is the pressure.

Figure 6a, b, respectively show the variability of T_{100} with water vapor mixing ratio at 100 hPa and 82 hPa and saturation mixing ratio (γ_{satt}) at 100 hPa estimated using the MLS measurements for the NH (top panel) and SH (bottom panel) hemispheres. The monthly mean tropopause height is considered at 100 hPa, thus, T_{100} is considered to be monthly mean tropopause temperature (NG81). The distribution of the water vapour follows the temperature cycle, which is well expected. Over the ASM, the T_{100} is found to vary between 189 and 196 K and water vapor follows the temperature cycle which is well expected. It is also revealed from Fig. 6a that over the ASM when $T_{100} > 195$ K, the lower stratospheric water vapor (at 100–82 hPa) is more and it is generally observed during JJA. A lag of one month is observed between T_{100} and 82 hPa as explained earlier. The monthly variability of γ_{satt} over the ASM shows as high as 6–8 ppmv during JJA indicating the holding capacity of the water vapor at 100 hPa. Moreover, the overshooting convective air parcel with relatively large water vapor can cross the tropopause only during the month of August, when the T_{100} is warmer (>195 K).

The EASM also shows similar variability as that of the ASM, however the water vapor available in the lower stratosphere is more compared to that of the ASM. This may be due to the fact the T_{100} is found to be as high as 198 K and γ_{satt} is found to be 12–15 ppmv which is much more than that of the ASM. The AM, the another northern

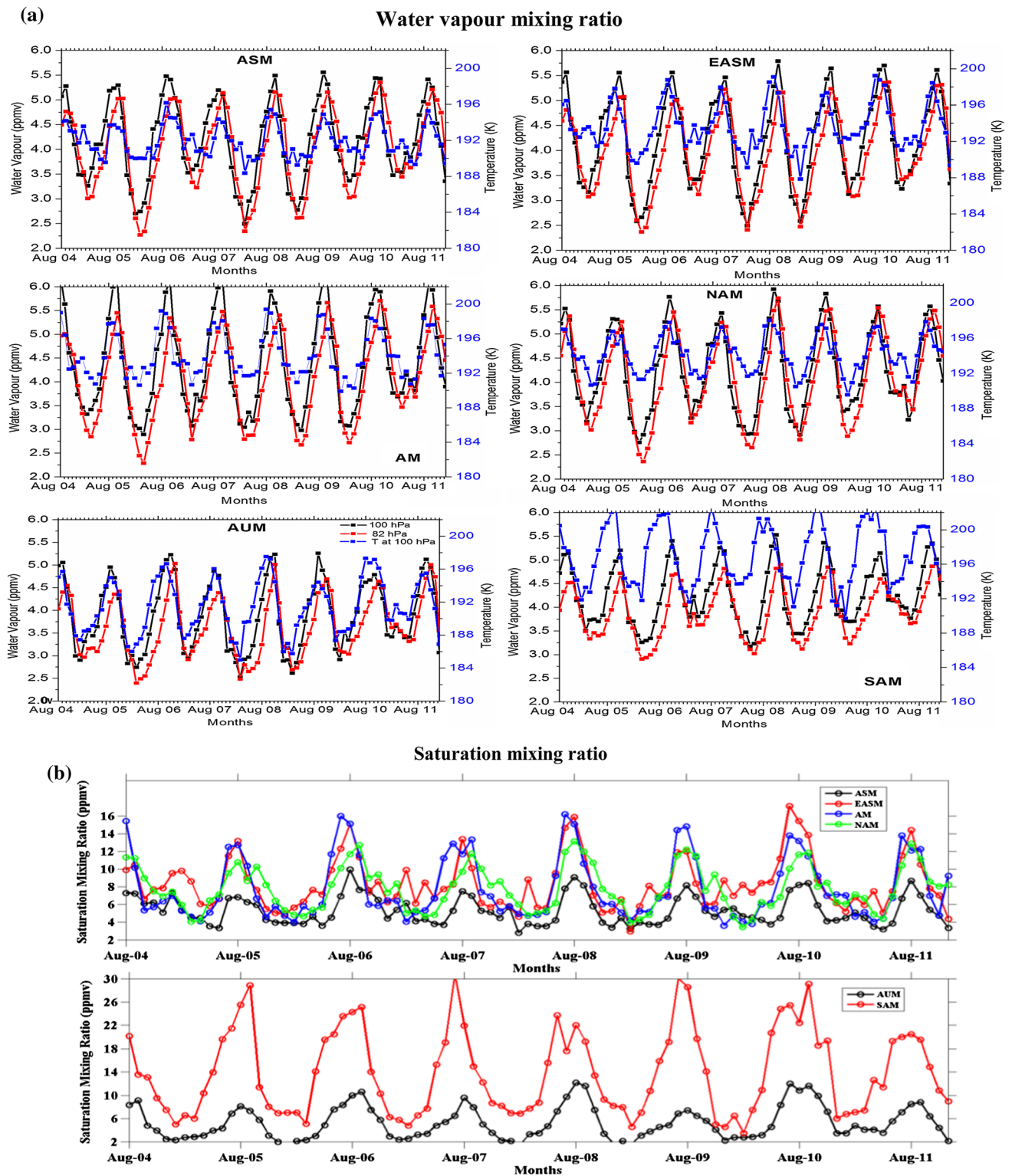


Fig. 6 **a** Monthly variability of water vapour mixing ratio at 100 and 82 hPa with temperature at 100 hPa and **b** saturation mixing ratio at 100 hPa over ASM, EASM, AM, NAM, AUM, and SAM

hemispheric monsoon season, shows considerably higher water vapor concentration in the lower stratosphere as compared to other monsoon regions (ASM and EASM).

The water vapor is found to be 6.1 ppmv at the tropopause which is ~ 1 ppmv higher than the ASM and 0.5 ppmv higher than the EASM. The T_{100} is found to be greater than

198 K. The concentration of water vapor at 82 hPa is 0.5 ppmv less than that of 100 hPa. The γ_{satt} is also observed to be high over the AM (14–15 ppmv) indicating that it can transport more water vapor to the stratosphere compared to the other monsoon region. The NAM region behaves similar to that of the ASM, except during 2006, 2008 and 2009, where the water vapor is found to be high (0.5 ppmv) compared to the other years. The seasonal variability in the temperature is found to vary between 191 and 197 K. The γ_{satt} over the NAM is observed to be about 10–11 ppmv. The holding capacity of water vapor is observed to be less over the ASM compared to the other monsoon regions, indicating that the tropopause is cool (as discussed in earlier section) over the ASM, which might lead to relatively more dehydration of water vapor over this region.

Over the SH monsoon regions, the T_{100} at the SAM shows as high as 202 K during the month of August, which is not observed over any other monsoon regions. The maximum temperature over the AUM is about 196 K, which is observed during the month of August. The water vapor at 100 hPa is found to be ~ 5 ppmv over the AUM and about 5.2–5.5 ppmv over the SAM. At 82 hPa, the water vapor is found to be 1 ppmv less than that of 100 hPa over both the monsoon regions. The γ_{satt} is observed to be high over the SAM compared to that of AUM but the availability of water vapor in the lower troposphere is less compared to the other monsoon regions. The above analysis indicate that even though the holding capacity of water vapor is observed to be high at the tropopause, the availability of water vapor at and above the tropopause is about 5–6 ppmv. It gives additional evidence that much water vapor is dehydrated well below the tropopause. Also over the ASM, where the availability of water vapor is almost twice than that of other regions, James et al. (2008) have shown that the air parcels are lifted by convection over the Bay of Bengal and Sea of China transported through the TTL via the monsoon anticyclonic circulation towards the North West India and gets eventually dehydrated. However the present analysis on the other hand shows that, within the TTL itself the water vapor gets dehydrated and the remaining water vapor only must have transported by advection. This is also found to be true for almost all the monsoon regions shown in the present study and the concentration is also found to be almost same (except at AM) at the tropopause level. The AM region is observed to be hydrating the stratosphere more compared to that of other monsoon regions and 1–1.5 ppmv difference is observed in the concentration.

One more interesting fact is that the maximum water vapor at the bottom of the TTL is found to be high during DJF over the AUM and SAM, however the pumping into the stratosphere is observed only during the month of

August, when the temperature at 100 hPa is highest. The above analysis suggests that water vapor enters the stratosphere during the months when the tropopause temperature is warmer, irrespective of the availability of the water vapor at the bottom of the TTL and different hemisphere monsoon regions.

4.2 Role of vertical convection

To get further insight for the role of convection in transport of the water vapor from lower troposphere to the UTLS region, the vertical velocity derived from the ERA-Interim reanalysis data have been plotted. Figure 7 shows the height-monthly variability and seasonal profiles of vertical velocity along with the monthly variability of the OLR over the ASM, EASM, AM, NAM, AUM and SAM. Relatively strong updrafts of $\sim 1.5 \text{ cm s}^{-1}$ are observed during JJA over the ASM and EASM and moderate updrafts of $\sim 0.75 \text{ cm s}^{-1}$ over AM, which is maximum around 12–14 km. Over the NAM, plume updrafts of $\sim 0.5 \text{ cm s}^{-1}$ are observed at 2 km and throughout the remaining troposphere the vertical velocity is closed to zero during JJA. During DJF, updrafts are observed over the AUM and SAM and their magnitude is $\sim 1 \text{ cm s}^{-1}$, which is maximum around 12–14 km. Thus the above analysis shows that the presence of updrafts in the upper troposphere over all the hemispheric monsoon regions, except for NAM during JJA and the maximum updraft is observed over the ASM. All the monsoon regions except the NAM, shows upward vertical velocity whenever $\text{OLR} < 220 \text{ W m}^{-2}$. Over the NAM, the OLR is always $> 240 \text{ W m}^{-2}$ which is also reflected in the vertical velocity plot i.e. absence of updraft. Accompanied with the updrafts downdrafts are also observed over the NH monsoon region during DJF and SH region during JJA. The magnitude of downdrafts were also found to be more (-1 cm s^{-1}) for the ASM compared to other monsoon regions and it is maximum in the mid-troposphere. The monsoon location where the updraft were stronger, viz., ASM, and EASM, during JJA, the water vapor concentration at 316–147 hPa are also high during that season. For the monsoon location in the NH where the updrafts are relatively weaker viz. NAM, the water vapor concentration is comparably low at 316–147 hPa. Over the SH also the updrafts are weak over the SAM compared to that of the AUM and the concentration of the water vapor also reflects the same. This analysis reveals the fact that the role of convection in transporting the water vapor from lower to middle troposphere and the concentration of water vapor transported depends on the intensity of convection (i.e. reflected in updraft and OLR). The interesting point to be noted is that even though the water vapor concentration is high in the middle troposphere (315–147 hPa) along with

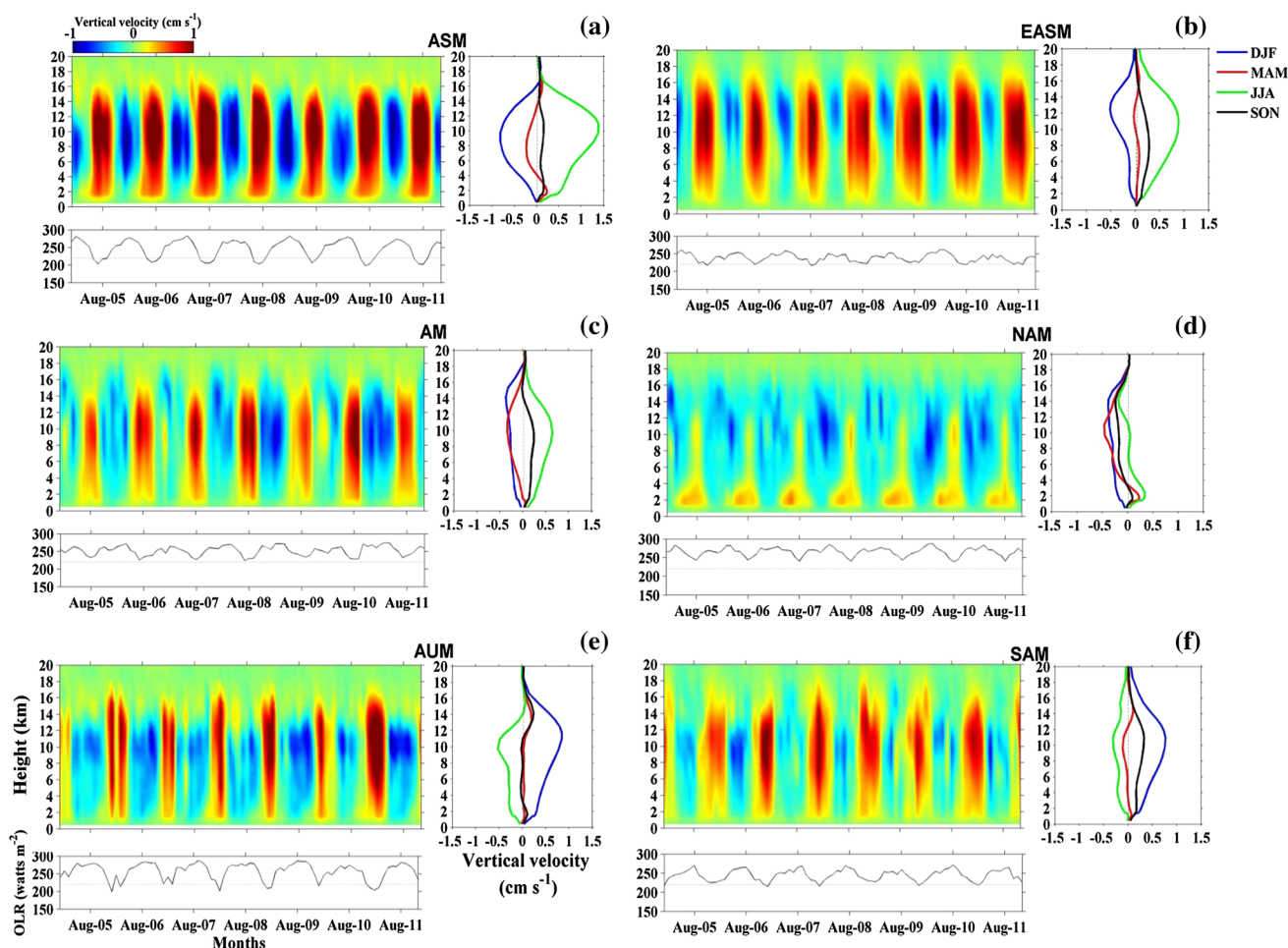


Fig. 7 Height-month variability (*left panels*), seasonal mean height profiles of vertical velocity (*right panels*), and OLR (*bottom panels*) over the a ASM, b EASM, c AM, d NAM, e AUM and f SAM regions, respectively

persistence of strong updraft throughout the troposphere, the concentration of water vapor transported to the lower and middle stratospheric region (100–82 hPa) remains to be the same for all the locations. The above also analysis reveals that the direct overshooting convection play a significant role in transporting the water vapor from lower to middle troposphere (up to 121 hPa) and have a limited role in transporting the water vapor from the upper troposphere to the lower stratosphere. Over the NAM, where the updraft is observed to be much weaker, the transport to the lower stratosphere may be due to slow diabatic ascent or through horizontal advection.

4.3 Role of horizontal advection

Apart from the vertical transport, there may be a possible role of horizontal advection in redistribution of water vapor in the vicinity of tropopause. Figure 8 shows the seasonal mean for JJA (*left panels*) and DJF (*right panels*) (averaged for 2004–2011) of water vapor mixing ratio with wind

vectors and upward vertical velocity ($>0.5 \text{ cm s}^{-1}$) (magenta colour closed contours) at different levels (stamped on figures). In the lower height region, i.e. at 261 hPa, the water vapor is pumped via over shooting convection indicated by the presence of updraft during JJA as discussed above. But above this height region, i.e. at 146 and 100 hPa, the outflow of the corresponding background winds redistributes or spread the water vapor from the monsoon regions, especially from the ASM and EASM region, where the tropical easterly jet is prominent (Das et al. 2011). The TEJ is widely distributing the water vapor to the western Arab regions and to the Northern and central parts of the African region at 150 and 100 hPa. This indicates that over the NAM, the distribution of water vapor above the tropopause is mainly due to the advection from the ASM region. It is to be noted that relatively lesser amount of water vapor is only transported vertically to the above regions because the presence of anticyclone in the vicinity of tropopause, traps the water vapor over the ASM. The wider distribution of water vapor over the AM region

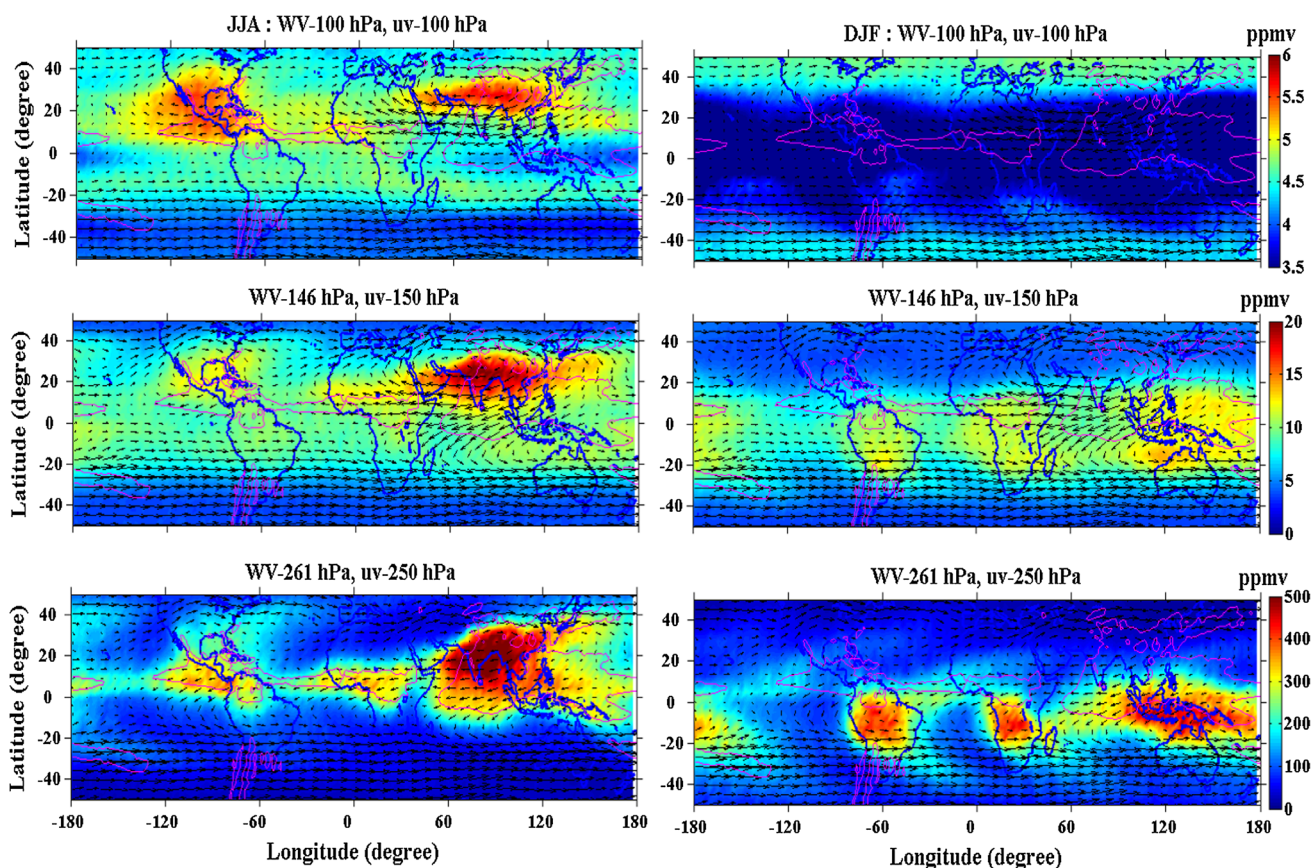


Fig. 8 Seasonal mean for JJA (*left panels*) and DJF (*right panels*) (2004–2011) of water vapour mixing ratio with wind vectors at different levels (stamped on figures) and upward vertical velocity ($>0.5 \text{ cm s}^{-1}$) (magenta colour closed contours) at 250 hPa

may be due to the trapping of water vapor by strong horizontal winds creating a closed circulation (shown in Fig. 8). It may also be due to rapid vertical transport of water vapor through convection or due to jumping cirrus and subsequent sublimation of ice clouds (Wang 2003). During DJF over the southern hemisphere, the water vapor is uniformly distributed at 146 hPa. It is found that the impact of horizontal advection is found to be weaker over the SH compared to that of the NH monsoon regions. At 100 hPa the water vapor is found to be very less and a spatially uniform distribution is observed during DJF.

4.4 Role of ice formation in dehydration

In addition to vertical and horizontal transport, ice sublimation or cirrus shooting can also contribute to the hydration or dehydration of the tropical lower stratosphere. Flury et al. (2012) have pointed out that an increase in the temperature in the TTL increases water vapor but decreases ice water content (IWC) and hence a balance is required between these two parameters. Therefore, the other components that must be investigated in view of transport and dehydration of the water vapor is the IWC relation with the

water vapor. Figure 9 shows the scatter plots between IWC and water vapor at 100 hPa for the ASM, EASM, AM, NAM, AUM and SAM. The IWC has a more useful meaning on the amount of water measured. The IWC is given in mg m^{-3} and water vapor in ppmv. If the temperature at 100 hPa is 195 K, 0.1 mg m^{-3} of ice corresponds to ~ 1 ppmv of water vapor using the ideal gas equation. Monthly mean for every year are taken and averaged over the domain mentioned in Sect. 2 for all the monsoon regions (JJA for the NH and DJF for the SH). The ASM and AUM shows the strongest anticorrelation (-0.6 and -0.7) compared to the other monsoon regions in the NH and the SH, respectively except the AM and EASM, which shows a weak positive correlation. Flury et al. (2012) have observed a strong anticorrelation in the tropics between water vapor and IWC. The strong anticorrelation suggests that the water vapor present at 100 hPa gets totally condensed to ice, thereby dehydrating the water vapor. This dehydration is found to be more over the ASM and AUM. The dehydration is basically because of the presence of cirrus, which is more prominent over the ASM and AUM during their respective monsoon seasons, as IWC can be taken as fraction of cirrus. Wang and Dessler

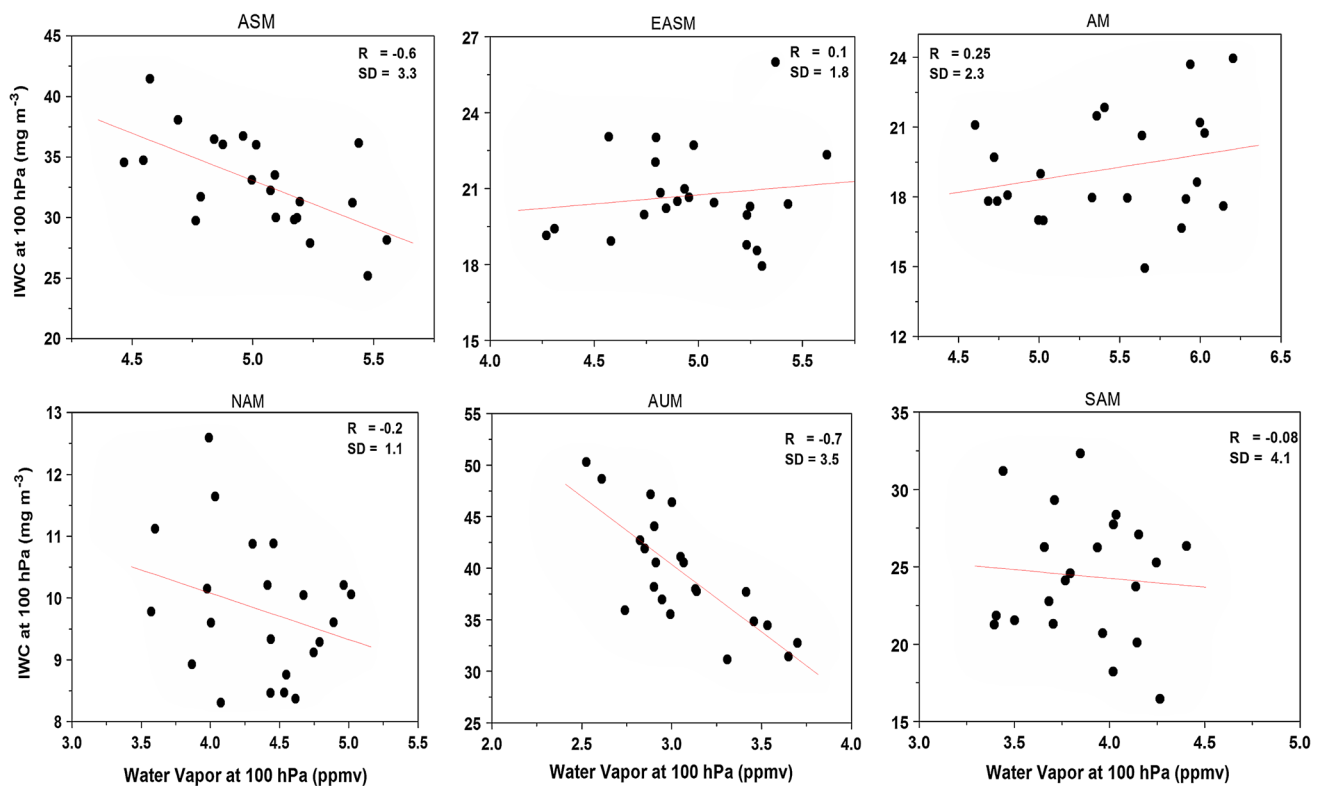


Fig. 9 Scatter plots between the IWC and water vapour at 100 hPa for ASM, EASM, AM, NAM, AUM and SAM, respectively

(2012) using CALIPSO data (2008–2010) showed that about 30 % of cirrus is of convective origin over the ASM and SAM regions. The cirrus fraction is generally high during DJF over the Northern Australia and during JJA over the monsoon regions of Asia and North America (Flury et al. 2012; Das et al. 2011). On the other hand the poor positive correlation over the AM (0.25) and the EASM (0.1), suggests that the total water vapor present at the tropopause is not getting fully condensed to ice, leaving behind little amount of water vapor that gets transported to the stratosphere. This could be the reason for AM to have high water vapor in the stratosphere compared to the other monsoon regions as discussed earlier. Over the SAM and NAM, the poor anticorrelation may be due to the fact that the tropopause temperature might be playing a role in controlling the transport to the stratosphere apart from the cirrus cloud cover. The cirrus cloud fraction is also very small over the SAM region (Wang and Dessler 2012). It is found that the AM and EASM in the NH is hydrating the stratosphere compared to the other monsoon regions where the water vapor gets dehydrated. Thus, the present results suggest the impact of different processes on the hydration and dehydration of the stratosphere over the different monsoon regions in both NH and SH regions. The analysis reflects that the AM and EASM hydrates the stratosphere with AM being higher compared to the other monsoon

regions. It is envisaged that the present study will have important implications as water vapor distribution in the UTLS regions influences the balance of planetary radiation and also in the UTLS chemistry over these monsoon regions.

5 Summary and concluding remarks

Eight years (2004–2011) of the Aura-MLS observations have been utilized to understand the hydration and the dehydration mechanism over the different northern and the southern hemispheric monsoon regions. The monsoon regions considered are the Asian Summer Monsoon, East Asian Summer Monsoon, Arizona Monsoon, North African Monsoon, South American Monsoon and the Australian Monsoon. The annual cycle of water vapor shows maxima during June–July–August over the NH and during December–January–February over the SH. The rate of air parcel travelling from the tropopause to the lower stratosphere is faster than from the lower to middle stratosphere. In addition, the air parcel moves with relatively faster in the NH compared to that of the SH in the lower stratosphere and vice versa in the middle stratosphere. The analysis revealed that the concentration of water vapour do not show much changes in the lower stratosphere over these

8 years. It is also observed that irrespective to the availability of the water vapor at the bottom of the TTL, the pumping of water vapor into the lower stratosphere is observed only during the month of August when the tropopause temperature is higher, suggesting the role of the tropopause temperature. It is also observed that the direct overshooting convection plays a significant role in transporting the water vapor from lower to the middle troposphere, however not much effective in transporting water vapor from upper troposphere to the lower and middle stratosphere, from where the moist adiabatic ascent dominates. Analysis also reveals that the water vapor is uniformly distributed at and above 146 hPa due to outflow of corresponding background wind. It is observed that moist adiabatic ascent transports the water vapor from the upper troposphere to the tropopause through moist adiabatic ascent over the ASM and EASM. On the other hand horizontal advection from the ASM transports to the UTLS region of the NAM. Further over the AM, the wide spread distribution at the tropopause is attributed to the rapid vertical transport through convection or to jumping cirrus and subsequent sublimation of ice clouds. Over the SH, both the convection and moist adiabatic ascent play a role, however the role of horizontal advection is observed to be negligible. The correlation analysis of the UTLS water vapor with temperature and ice water content shows that the AM and EASM, with the AM being high, is hydrating the stratosphere compared to all the other monsoon regions where the water vapor is getting dehydrated. Thus the present results will have important implications in understanding the exchange processes across the tropopause over the different monsoon regions.

Acknowledgments The Aura-MLS data are downloaded from the Goddard Earth Sciences Data and Information Services Centre, the ERA-Interim from the ECMWF and the gridded OLR from the NOAA-CIRES. The authors are thankful to the Director, SPL/VSSC for his constant support. Finally, the author would like to thank the Editor and the two anonymous reviewers for their constructive comments and suggestions which improve the manuscript greatly.

References

Adams DK, Comrie AC (1997) The North American Monsoon. *Bull Amer Meteor Soc* 78: 2197–2213
 Bannister RN, O’Neill A, Gregory AR, Nissen KM (2004) The role of the South-East Asian monsoon and other seasonal features in creating the ‘tape recorder’ signal in the unified model. *Q J R Meteorol Soc* 130:1531–1554. doi:10.1256/qj.03.106
 Bolton D (1980) The computation of equivalent potential temperature. *Mon Wea Rev* 108:1046–1053
 Brewer AW (1949) Evidence for a world circulation provided by the measurements of helium and water vapour distribution in the stratosphere. *Quar J R Met Soc* 75:351–363
 Das SS (2009) A new perspective on MST radar observations of stratospheric intrusions into troposphere associated with tropical

cyclone. *Geophys Res Lett* 36:L15821. doi:10.1029/2009GL039184
 Das SK, Chiang CW, Nee JB (2011) Influence of tropical easterly jet on upper tropical cirrus: an observational study from CALIPSO, Aura-MLS, and NCEP/NCAR data. *J Geophys Res* 116. doi:10.1029/2011JD015923D12204
 Davidson E, Bride Mc, McAvaney BJ (1983) The onset of Australian monsoon during winter MONEX: synoptic aspects. *Mon Wea Rev* 111:496–516
 Dee DP et al (2011) The ERA-Interim reanalysis: configuration and performance of the data assimilation system. *Quart J R Meteorol Soc* 137:553–597. doi:10.1002/qj.828
 Dessler AE, Kim H (1999) Determination of the amount of water vapour entering the stratosphere based on Halogen Occultation Experiment (HALOE) data. *J Geophys Res* 104:30605–30607
 Devasthale A, Fueglistaler S (2010) A climatological perspective of deep convection penetrating the TTL during the Indian summer monsoon from the AVHRR and MODIS instruments. *Atmos Chem Phys* 10:4573–4582
 Dvortsov VL, Solomon S (2001) Response of the stratospheric temperatures and ozone to past and future increases in stratospheric humidity. *J Geophys Res* 106(D7):7505–7514. doi:10.1029/2000JD900637
 Flury T, Wu DL, Read WG (2012) Correlation among cirrus ice content, water vapour and temperature in the TTL as observed by CALIPSO and Aura/MLS. *Atmos Chem Phys* 12:683–691
 Froidevaux I, Livesey NJ, Read WG, Jiang YB, Jimenez C, Filipiak MJ et al (2006) Early validation analyses of atmospheric profiles from EOS MLS on the AURA satellite. *IEEE Trans Geosci Remote Sens* 44(5):1106–1121
 Fu R, Hu Y, Wright JS, Jiang JH, Dickinson RE, Chen M et al (2006) Short circuit of water vapour and polluted air to the global stratosphere by convective transport over the Tibetan Plateau. *Proc Natl Acad Sci USA* 103(15):5664–5669
 Fueglistaler S, Bonazzola M, Haynes PH, Peter T (2005) Stratospheric water vapour predicted from the Lagrangian temperature history of air entering the stratosphere in the tropics. *J Geophys Res* 110:D08107. doi:10.1029/2004JD005516
 Fueglistaler S, Dessler A, Dunkerton T, Folkins I, Fu Q, Mote P (2009) Tropical tropopause layer. *Rev Geophys* 47:1004. doi:10.1029/2008RG000267
 Fujinami H, Nomura S, Yasunari T (2005) Characteristics of diurnal variations in convection and precipitation over the southern Tibetan Plateau during summer. *SOLA* 1:49–52. doi:10.2151/sola.2005-014
 Gettelman A, Salby ML, Sassi F (2002) The distribution and influence of convection in the tropical tropopause region. *J Geophys Res* 107(D10):4080. doi:10.1029/2001JD001048
 Hastenrath S (2000) Interannual and longer term variability of upper-air circulation over the tropical Atlantic and west Africa in boreal summer. *Int J Clim* 20:1415–1430
 Hirose M, Nakamura K (2005) Spatial and diurnal variations of precipitation systems over Asia observed by the TRMM Precipitation Radar. *J Geophys Res* 110:D05106. doi:10.1029/2004JD004815
 Holton JR, Gettelman A (2001) Horizontal transport and dehydration in the stratosphere. *Geophys Res Lett* 28:2799–2802
 Holton JR, Haynes PH, McIntyre ME, Douglass AR, Rood RB, Pfister L (1995) Stratosphere–troposphere exchange. *Rev Geophys* 33:403–439
 James R, Bonazzola M, Legras B, Surbled K, Fueglistaler S (2008) Water vapour transport and dehydration above convective outflow during Asian monsoon. *Geophys Res Lett* 35. doi:10.1029/2008GL035441L20810
 Lambert A, Read WG, Livesey NJ, Santee ML, Manney GL, Froidevaux L, Lambert D et al (2007) Validation of the Aura

- Microwave Limb Sounder stratospheric water vapour and nitrous oxide measurements. *J Geophys Res* 112(D24):D24S36. doi:[10.1029/2007JD008724](https://doi.org/10.1029/2007JD008724)
- Lelieveld J, Brühl C, Jöckel P, Steil B, Crutzen PJ, Fischer H, Lelieveld J et al (2007) Stratospheric dryness: model simulations and satellite observations. *Atmos Chem Phys* 7:1313–1332
- Liebmann B, Smith CA (1996) Description of a complete interpolated outgoing long wave radiation dataset. *Bull Am Meteor Soc* 77:1275–1277
- Liu C, Zipser E, Garrett T, Jiang JH, Su H (2007) How do the water vapour and carbon monoxide “tape recorders” start near the tropical tropopause? *Geophys Res Lett* 34. doi:[10.1029/2006GL029234](https://doi.org/10.1029/2006GL029234)
- Livesey NJ, Read WG, Froidevaux L, Lambert A, Manney GL, Pumphrey HC et al (2011) EOS MLS version V3.3 level 2 data quality and description document. Jet Propul. Lab., Pasadena, CA. <http://mls.jpl.nasa.gov>
- Mote PW, Rosenlof KH, McIntyre ME, Carr ES, Gille JC, Holton JR et al (1996) An atmospheric tape recorder. The imprint of tropical tropopause temperatures on stratospheric water vapour. *J Geophys Res* 101:3989–4006. doi:[10.1029/95JD03422](https://doi.org/10.1029/95JD03422)
- Newell RE, Gould Stewart S (1981) A stratospheric fountain? *J Atmos Sci* 38:2789–2796
- Park M, Randel WJ, Gettelman A, Massie ST, Jiang JH (2007) Transport above the Asian summer monsoon anticyclone inferred from Aura Microwave Limb Sounder tracers. *J Geophys Res* 112:D16309. doi:[10.1029/2006JD008294](https://doi.org/10.1029/2006JD008294)
- Petersen WA, Rutledge SA (2001) Regional variability in tropical convection: observations from TRMM. *J Clim* 14:3566–3586
- Randel WJ, Moyer E, Park M, Jensen E, Bernath P, Walker K, Boone C (2012) *J Geophys Res* 117. doi:[10.1029/2011JD016632](https://doi.org/10.1029/2011JD016632)
- Rao TN, Uma KN, Rao DN, Fukao S (2008) Understanding the transportation process of tropospheric air entering the stratosphere from direct vertical air motion measurements over Gadanki and Kototabang. *Geophys Res Lett* 35:L15805. doi:[10.1029/2008GL034220](https://doi.org/10.1029/2008GL034220)
- Read WG, Lambert A, Bacmeister J, Cofield RE, Christensen LE, Cuddy DT et al (2007) EOS Aura Microwave Limb Sounder upper tropospheric and lower stratospheric humidity validation. *J Geophys Res* 112:D24S35. doi:[10.1029/2007JD008752](https://doi.org/10.1029/2007JD008752)
- Rosenlof KH, Chiou EW, Chu WP, Johnson DG, Kelly KK, Michelsen HA, Nedoluha GE, Remsberg EE, Toon GC, McCormick MP (2001) Stratospheric water vapour increases over the past half-century. *Geophys Res Lett* 28:1195–1198. doi:[10.1029/2000GL012502](https://doi.org/10.1029/2000GL012502)
- Schneider T, O’Gorman PA, Levine XJ (2010) Water vapour and the dynamics of climate changes. *Rev Geophys* 48:RG3001. doi:[10.1029/2009RG000302](https://doi.org/10.1029/2009RG000302)
- Schwartz MJ et al (2008) Validation of the Aura Microwave Limb Sounder temperature and geopotential height measurements. *J Geophys Res* 113:D15S11. doi:[10.1029/2007JD008783](https://doi.org/10.1029/2007JD008783)
- Shindell DT (2001) Climate and ozone response to increased stratospheric water vapour. *Geophys Res Lett* 28:1551–1554
- Solomon S, Rosenlof KH, Portmann RW, Daniel JS, Davis SM, Sanford TJ, Plattner GK (2010) Contributions of stratospheric water vapour to decadal changes in the rate of global warming. *Science* 327:1219–1223. doi:[10.1126/science.1182488](https://doi.org/10.1126/science.1182488)
- Tetens O (1930) Über einige meteorologische Begriffe. *Z. Geophys.* 6:297–309
- Uma KN, Das SK, Kumar KK (2013) Aura-MLS observations of water vapour entering the stratosphere over the Northern Bay of Bengal and East Equatorial Indian Ocean. *Terr Atmos Ocea Sci* 24(3):357–368. doi:[10.3319/TAO.2012.11.06.01\(A\)](https://doi.org/10.3319/TAO.2012.11.06.01(A))
- Uyeda H, Yamada H, Horikomi J, Shirooka R, Shimizu S, Liu L, Ueno K, Fujii H, Koike T (2001) Characteristics of convective clouds observed by a Doppler radar at Naqu on Tibetan Plateau during the GAME-Tibet IOP. *J Meteorol Soc Jpn* 79(1B):463–474
- Wang PK (2003) Moisture plumes above thunderstorm anvils and their contributions to cross tropopause transport of water vapour in midlatitudes. *J Geophys Res* 108:4194. doi:[10.1029/2002JD002581](https://doi.org/10.1029/2002JD002581)
- Wang T, Dessler AE (2012) Analysis of cirrus in the tropical tropopause layer from CALIPSO and MLS data: a water perspective. *J Geophys Res* 117:D04211. doi:[10.1029/2011JD016442](https://doi.org/10.1029/2011JD016442)
- Waters JW, Froidevaux L, Jarnot RF, Pickett HM, Read WG, Siegel PH et al (2006) The Earth Observing System Microwave Limb Sounder (EOS MLS) on the Aura satellite. *IEEE Trans Geosci Remote Sens* 44:1075–1092. doi:[10.1109/TGRS.2006.873771](https://doi.org/10.1109/TGRS.2006.873771)
- Wright JS, Fu R, Fueglistaler S, Liu Y, Zhang Y (2011) The influence of summertime convection over South-East Asia on water vapour in the tropical stratosphere. *J Geophys Res* 116:D12302. doi:[10.1029/2010JD015416](https://doi.org/10.1029/2010JD015416)
- Yasunari T, Miwa T (2006) Convective cloud systems over the Tibetan Plateau and their impact on mesoscale disturbances in the Meiyu/Baiu frontal zone. *J Meteorol Soc Jpn* 84(4):783–803
- Zeng X, Lu E (2004) Globally unified monsoon onset and retreat indices. *J Clim* 17:2241–2248
- Zhou JY, Lau KM (1999) Does a monsoon climate exist over South America? *J Clim* 11:1020–1040